Evolution of the plankton paleome in the Black Sea from the Deglacial to Anthropocene

Marco J. L. Coolen[a,1], William D. Orsi[b], Cherel Balkema[a], Christopher Quince[c], Keith Harris[c], Sean P. Sylva[a], Mariana Filipova-Marinova[d], and Liviu Giosan[b]

[a]Marine Chemistry and Geochemistry Department and [b]Geology and Geophysics Department, Woods Hole Oceanographic Institution, Woods Hole, MA 02543; [c]School of Engineering, Glasgow University, Glasgow G12 8LT, United Kingdom; and [d]Museum of Natural History, 9000 Varna, Bulgaria

Edited by Katherine H. Freeman, The Pennsylvania State University, University Park, PA, and accepted by the Editorial Board April 10, 2013 (received for review November 7, 2012)

The complex interplay of climate shifts over Eurasia and global sea level changes modulates freshwater and saltwater inputs to the Black Sea. The dynamics of the hydrologic changes from the Late Glacial into the Holocene remain a matter of debate, and information on how these changes affected the ecology of the Black Sea is sparse. Here we used Roche 454 next-generation pyrosequencing of sedimentary 18S rRNA genes to reconstruct the plankton community structure in the Black Sea over the last ca. 11,400 y. We found that 150 of 2,710 species showed a statistically significant response to four environmental stages. Freshwater chlorophytes were the best indicator species for lacustrine conditions (>9.0 ka B.P.), although the copresence of previously unidentified marine taxa indicated that the Black Sea might have been influenced to some extent by the Marmara Sea since at least 9.6 ka calendar (cal) B.P. Dinoflagellates, cercozoa, eustigmatophytes, and haptophytes responded most dramatically to the gradual increase in salinity after the latest marine reconnection and during the warm and moist mid-Holocene climatic optimum. According to paired analysis of deuterium/hydrogen (D/H) isotope ratios in fossil alkenones, salinity increased rapidly with the onset of the dry Subboreal after ∼5.2 ka B.P., leading to an increase in marine fungi and the first occurrence of marine copepods. A gradual succession of dinoflagellates, diatoms, and chrysophytes occurred during the refreshening after ∼2.5 ka cal B.P. with the onset of the cool and wet Subatlantic climate and recent anthropogenic perturbations.

amplicon pyrosequencing | ancient plankton DNA | *D/H* ratios in alkenones | paleoenvironment

The semi-isolated Black Sea is highly sensitive to climate-driven environmental changes, and the underlying sediments represent high-resolution archives of past continental climate and concurrent hydrologic changes in the basin. A positive freshwater budget controlled by tributary rivers and direct precipitation leads to low-salinity water export toward the Mediterranean through the narrow and shallow Straits of Bosporus. Denser water from the Sea of Marmara flows into the Black Sea as an undercurrent. The permanently stratified Black Sea is the largest anoxic basin in the world, and an ∼30-m-thick suboxic zone separates the sulfidic bottom waters from the upper ∼100 m of oxygenated surface waters. During glacial sea level lowstands, the marine connection was hindered, and the Black Sea functioned as a giant lake (1).

Two opposing scenarios have been proposed to explain the most recent transition of the Black Sea from lacustrine to marine environment: a "catastrophic" postglacial flooding of the Black Sea with Mediterranean waters (2, 3) and a "gradual marine reconnection" (1, 4). A sharp change from lacustrine to marine conditions characterizes slope and basin sedimentary records in highly sensitive geochemical proxies, such as the strontium isotope composition of carbonate shells (5). This initial marine inflow (IMI) was recently calibrated to 9.0 ka calendar (cal) B.P. after correction for reservoir age (6). Despite the lack of evidence of a marine water source, whether the Black Sea was fresh or brackish before the marine reconnection is a matter of ongoing debate. The chloride content and stable oxygen isotope ($\delta^{18}O$) composition of sediment interstitial water suggest that the Late Glacial (Neoeuxinian) Black Sea was a freshwater lake (7), whereas the fossil dinocyst assemblage implies brackish conditions [i.e., a salinity of ∼7–12 parts per thousand (ppt)] (8). Furthermore, the oxygen isotopic composition of fossil *Dreissena* shells suggests an increase in sea surface salinity (SSS) during the Bølling-Allerød and Preboreal warm oscillations (9).

Although the strontium isotopic record does not support an inflow of marine waters before 9 ka cal B.P. (5), much of the $\delta^{18}O$ shift in biogenic carbonates might be explained by excess evaporation during dry glacial and deglacial intervals (5, 10). Hydrologic changes in the Black Sea after the marine reconnection are controversial as well. Modeling (7) and micropaleontologic reconstructions (8, 11, 12) agree on a gradual salinization of the Black Sea, but the establishment of modern-day hydrologic conditions is not well constrained ecologically and chronologically. For example, the thin aragonite layers located at the bottom of the organic-rich Holocene sapropel are characterized by the presence of marine calcareous nannofossils (11), and the concomitant disappearance of fresh-to-brackish ostracods and bivalves (9, 10, 13) possibly mark the onset of modern-day hydrologic conditions at ∼7.5 ka cal B.P. Alternatively, the dominance of euryhaline dinoflagellates has been considered to mark modern-day conditions in the Black Sea after ∼5.6 ka B.P. (8). Furthermore, the chloride and $\delta^{18}O$ composition of sediment interstitial water suggests that modern hydrologic conditions were established only 1,500–2,500 y ago (7), concomitant with the start of deposition of calcareous coccoliths of the haptophyte *Emiliania huxleyi* (11). Paleoenvironmental interpretations from calcareous or siliceous microfossils are often complicated by dissolution processes, however; moreover, the majority of plankton, including 80% of dinoflagellate species, do not produce fossilizing cellular diagnostic features (14) and escape identification in the fossil record. In addition, salinity reconstructions based on $\delta^{18}O$ ratios are hampered by the absence of planktonic foraminifera preserved in Black Sea sediments.

The analysis of genetic signatures preserved in geological samples, recently defined as the paleome (15), makes use of the ability to include key paleoenvironmental indicator species that leave no other diagnostic features in the sediment record (16–19). This is especially important given the recent report that the majority of DNA in marine sediments is extracellular (20), which implies that species identified in micropaleontological studies do not necessary

Author contributions: M.J.L.C., W.D.O., M.F.-M., and L.G. designed research; M.J.L.C., C.B., and S.P.S. performed research; M.J.L.C., W.D.O., and C.Q. contributed new reagents/analytic tools; M.J.L.C., W.D.O., C.Q., K.H., and L.G. analyzed data; and M.J.L.C. and L.G. wrote the paper.

The authors declare no conflict of interest.

This article is a PNAS Direct Submission. K.H.F. is a guest editor invited by the Editorial Board.

Data deposition: The sequences reported in this paper have been deposited in the GenBank database (accession nos. KC787374–KC787532).

[1]To whom correspondence should be addressed. E-mail: mcoolen@whoi.edu.

This article contains supporting information online at www.pnas.org/lookup/suppl/doi:10.1073/pnas.1219283110/-/DCSupplemental.

represent the most abundant past plankton members. To date, only low-throughput capillary sequencing-based molecular methods have been used to study sedimentary paleomes.

With access to a continuous, well-preserved sedimentary record from multicores and gravity cores retrieved at a water depth of 980 m off the Bulgarian coast in 2006, we reconstructed the past eukaryotic plankton members of the Black Sea in 48 sediment intervals spanning key climate stages over the last 11,400 y through pyrosequencing (21) of PCR-amplified sedimentary eukaryotic 18S rRNA genes. In addition, we reconstructed the postglacial distribution of copepods as potential environmental marker species, which normally do not leave useful diagnostic features in the sediment, from preserved fossil copepod 18S rRNA genes using a targeted PCR approach coupled with denaturing gradient gel electrophoresis (DGGE) (22) and capillary sequencing of individual DGGE fragments. We also compared past salinity values inferred from environmental indicator species identified from the paleome with SSS estimates from deuterium/hydrogen (D/H) isotope ratio values in fossil alkenones (23, 24). Our paired fossil DNA and molecular level isotopic measurements provide detailed insight into the Black Sea's plankton ecology and response to environmental changes occurring during key climatic stages and transitions from the Preboreal to the recent Anthropocene.

Results and Discussion

Sediment Chronology and Geochemistry. The geochemical, molecular isotopic, and paleomic datasets presented in this study were measured on radiocarbon-dated sediments from Giant Gravity Core (GGC) 18 and Multicore (MC) 19 (17, 24). Radiocarbon dating of individual organic compounds (25) has indicated that preaged detrital organic carbon is a minor component of the bulk organic carbon in Holocene Black Sea sediments. However, given our incomplete understanding of the time variability of detrital organic carbon inputs, and for consistency with previous studies, we applied the classical correction (26) to our organic carbon dates (17). Radiocarbon dates on carbonates from Unit III were calibrated using the latest reconstruction of Black Sea reservoir age (*SI Appendix*). The timing of diagnostic shifts in sedimentation (i.e., from calcium and organic carbon contents) correspond well with those reported previously. Oxygenated and total organic carbon (TOC)-poor (<0.5 wt% TOC) lacustrine sediments between ~11.4 and 9.4 ka cal B.P. are composed mainly of authigenically precipitated calcite (Unit III C1 interval) (Fig. 1*A*) (9, 13). The gray-green colored T interval (9), with an average TOC content of 2.4 ± 0.8 wt%, separates the calcite-rich C1 interval from the anoxic, organic-rich marine sapropel (27). The onset of Unit II or sapropel deposition at ~7.5 ka cal B.P. is indicated by the upper aragonite peak and by a steep increase in TOC to 15 wt% (Fig. 1 *A* and *B*). The uppermost laminated and organic-rich Unit I (3.8% ± 0.5% TOC) interval with abundant *E. huxleyi* coccoliths (28) was formed during the last 2,500 y (Fig. 1*A*). The undisturbed sapropel Unit II and laminated Unit I coccolith marl were deposited under permanent bottom water anoxia conditions and lack visible bioturbation.

This part of the GGC18 record was previously used for a paired fossil DNA and lipid biomarker survey to reconstruct the Holocene succession of haptophyte algae as sources of fossil long-chain alkenone lipid biomarkers (17), as well as to reconstruct viral infection of past *E. huxleyi* populations (19). The preservation of DNA in the anoxic TOC-rich marine sediments of GGC18 was excellent, as shown by the constant ratio between the amounts of refractory alkenones and ~500-bp-long fossil haptophyte 18S rRNA gene fragments (17). Interestingly, sedimentary DNA represented the largest fraction of total organic matter, notably in the most TOC-depleted lacustrine C1 interval (Fig. 1*B*). This suggests that ancient plankton also might be preserved in sediments that were deposited under well-mixed and oxygenated conditions.

In the present study, we used ancient DNA methods to reconstruct the past plankton composition from the late Pleistocene and early Holocene lacustrine and low-salinity Black Sea sediments of Unit III.

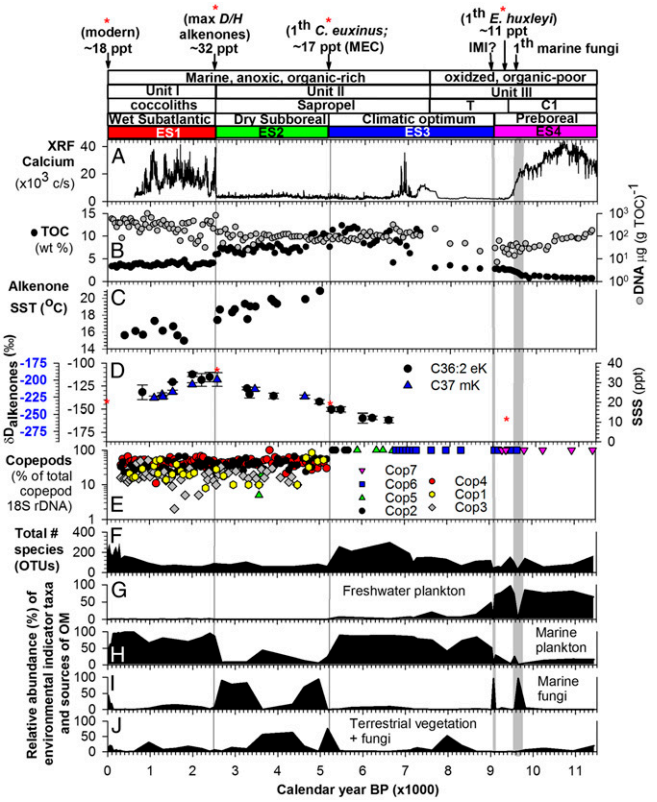

Fig. 1. (*A–C*) Postglacial sediment record of MC19 and GGC18 with calcium content, measured by X-ray fluorescence (XRF) scanning (*A*), TOC and DNA content (*B*), and alkenone SST (*C*) (17). (*D*) δD values of long-chain alkenones (i.e., C_{37} mK and $C_{36:2}$ eK) and estimated SSS values (24). (*E*) Relative abundance of seven copepod OTUs identified through copepod-specific PCR and capillary sequencing of individual DGGE fragments. Phylogenetic information on the recovered copepod sequences is provided in *SI Appendix*, Table S2. (*F–J*) Pyrosequencing dataset with number of OTUs per sample and the relative abundance of OTUs indicative of freshwater, marine, or terrestrial origin as inferred from the habitat of their most closely related sequences (*SI Appendix*, Figs. S5–S9). The timeline of events (i.e., changes in sedimentation type, climate stages, and environment, plus associated ecological changes) is denoted above all figures and explained in the text. Red asterisks denote SSS estimates from the first occurrence of *E. huxleyi* DNA (Fig. 3), and additional proxies listed above *A*.

Environmental Stages of the Black Sea. Four distinct environmental stages, designated ES1–ES4, were defined by three major environmental transitions (Fig. 1): the IMI at 9.0 ka cal B.P., the establishment of modern environmental conditions at ~5.2 ka cal B.P., and the onset of freshening at ~2.5 ka cal B.P. The ES4 lacustrine interval (~11.4–9.0 ka cal B.P.) spanning the relatively dry Preboreal (29) was followed by a period of slowly increasing SSS, corresponding to the warm and moist mid-Holocene climatic optimum (ES3) (29). The establishment of modern-day SSS was identified by the presence of preserved 18S rRNA genes of marine copepods (Fig. 1*E* and *Appendix S1*, Fig. S1 and Table S2).

Copepods have been excluded from previous paleoecological studies because the copepod material preserved in the underlying sediment record is mainly resting eggs, with poor diagnostic/taxonomic features (30). However, the arrival of marine copepods, most notably *Calanus euxinus* (clone Cop 4), with a minimum salinity tolerance of ~17 ppt (31), at ~5.2 ka cal B.P. marks the establishment of modern environmental conditions in the Black Sea. The ES2 interval (~5.2–2.5 ka cal B.P.) covers the dry and cooler Subboreal (29) and represents the peak of marine conditions in the Black Sea. During this time interval, the SSS increased steeply from ~17 ppt to a maximum of ~32 ppt as

inferred, from the *D*/*H* ratio of *E. huxleyi*-derived C_{37} methyl ketones (C_{37} mK) (Fig. 1*D*) as a quantitative SSS proxy (23, 24), whereas the average alkenone-derived sea surface temperature (SST) decreased gradually from ~20 °C to 16 °C (Fig. 1*C*) (17). Measurement of the *D*/*H* ratio of the *E. huxleyi*-specific $C_{36:2}$ ethyl ketone (eK) (32) corroborated this SSS history (Fig. 1*D*), further suggesting that the salinity was already ~14 ppt after deposition of the aragonite layers at the base of the sapropel (~6.6 ka cal B.P.), where δD C_{37} mK values are not reliable owing to a variable haptophyte assemblage (17). Earlier, at ca. 8 ka cal B.P., the Black Sea likely was not much fresher, as suggested by the disappearance of dinocysts of *Spiniferitus cruciformis* with a maximum salinity tolerance of ~12 ppt (12). The coccolith marl of Unit I represents the final environmental stage (ES1; final 2.5 ky), when, according to the alkenone *D*/*H* ratios, the Black Sea experienced a dramatic freshening throughout the entire basin (23, 24), which coincides with the onset of the Subatlantic climate (29).

Reconstructing the Black Sea Paleome. We used pyrosequencing of PCR-amplified sedimentary 18S rRNA genes to generate an overall window into the past plankton species and to refine our understanding of the ecological responses to environmental changes in the Black Sea since the deglacial. A total of 2,370 ± 1,092 high-quality sequences (340 bp long) from 48 samples were analyzed. Grouping sequences into operational taxonomic units (OTUs) sharing 97% sequence identity resulted in 50–350 OTUs per sample (Fig. 1*F* and *SI Appendix*, Fig. S2). We investigated the impact of the four environmental stages (described above), and the transitions between these stages, on the planktonic community structure using nonmetric multidimensional scaling (NMDS) (Fig. 2*A*). Samples were generally grouped based on environmental stages, and the stage transitions correspond to major changes in community structure. Groupings were highly significant ($P < 0.001$, permutational multivariate ANOVA), and 25% of the variance in community structure was explained by the environmental stage. Furthermore, indicator species analysis (ISA) (33) showed that 150 out of 2,710 unique OTUs responded significantly ($P < 0.05$) to the Holocene environmental changes in the Black Sea (Fig. 2 and *SI Appendix*, Table S3). The 150 indicator species identified belonged to Alveolata (notably Dinophyceae), Cercozoa, Fungi, Haptophyta, Ichthyosporea, Metazoa (bivalves), Stramenopiles (phototrophic Bacillariophyta, Bolidophyceae, Chrysophyceae, Dictyochophyceae, Eustigmatophytes, and heterotrophic Labyrinthulida), and Viridiplantae (Chlorophyta and Streptophyta) (*SI Appendix*, Figs. S3 and S4). Replotting the community NMDS using only these indicator species (Fig. 2*B*) revealed a stronger clustering with environmental stage.

Chlorophytes were the dominant group of eukaryotic plankton (48% of OTUs) for lacustrine sediments older than 9.0 ka cal B.P. Indicator species C5 was identical to *Choricystis* sp. Pic8/18P-11w (AY197629), isolated from the moderately eutrophic freshwater Picnic Pond in Itasca State Park, Minnesota (*SI Appendix*, Fig. S5), and was the most abundant OTU (Fig. 3) and best indicator species for ES4 [indicator value (IV) = 95, $P = 0.0002$] (Fig. 2*C* and *SI Appendix*, Table S3). Dinoflagellate OTU C57, with 99.7% sequence similarity to clone LG10-02 (AY919716) from freshwater Lake George (New York), was the second-best indicator for ES4 (Fig. 3 and *SI Appendix*, Fig. S6 and Table S3). *Dreissena* shells were previously recovered from Holocene coastal margin sediments of the Black Sea and have been used for $\delta^{18}O$ reconstructions (5). The 18S rDNA of this freshwater mussel (OTU C161) was also representative of ES4 (Fig. 3). Lacustrine plankton comprised ~65–98% of the eukaryote DNA pool in ES4 (Fig. 1*G*); however, the paleome of ES4 also consisted of marine plankton, such as coastal dinoflagellates. Most notably, *Scrippsiella trochoidea* (OTU C49), which is common in the Mediterranean Sea (34), composed up to 4% of the pyrotags, even in the oldest analyzed sediments of ES4 (Fig. 3). Furthermore, the decline in the relative abundance of lacustrine species at ~9.6 ka cal B.P. (Fig. 3 and *SI Appendix*, Figs. S3 and S7) coincides with the arrival of a marine fungus

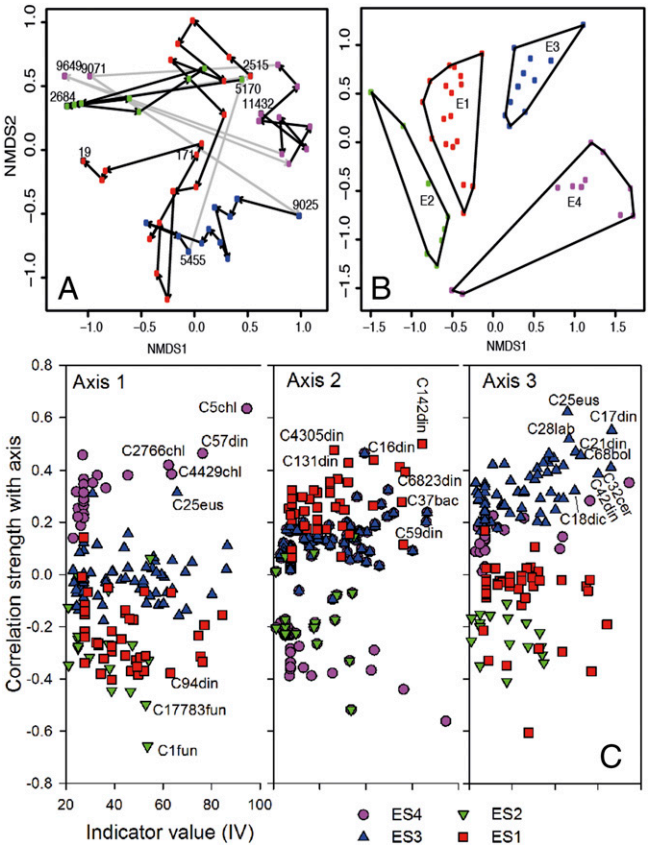

Fig. 2. (*A*) NMDS of community compositions using all 2,710 OTUs in 48 selected Black Sea sediments. Arrows indicate transitions in the time series, and selected times are labeled. (*B*) NMDS of community structure restricted to the 150 OTUs that demonstrated a statistically significant response to the environmental changes in the Black Sea according to an initial ISA using the statistical software package PC-ORD 5.0. (*C*) Relationships of species (i.e., OTU) correlation strength (*r*) with axes from the NMDS analysis and IVs from the ISA analysis. OTUs with the highest *r* values and IVs (i.e., the best environmental indicator species) are numbered in the panels. Details of indicator species and phylogenetic trees are provided in *SI Appendix*, Table S3 and Figs. S5–S9. Color code for circles: pink, ES4; blue, ES3; green, ES2; red, ES1.

(OTU C1) with 100% sequence identity to ascomycete fungi from the coastal Arabian Sea oxygen minimum zone (35). A second peak of the marine fungus occurred at the previously reported IMI at 9.0 ka cal B.P. *E. huxleyi* (C233) appeared in the Black Sea at ~9.3 ka cal B.P. (Fig. 3), which is ~1,800 y earlier than previously thought based on preserved coccoliths in the earliest aragonite peak at the base of the sapropel (11, 36).

A major shift in the plankton community structure occurred at the ES4/ES3 transition at ~9.0 ka cal B.P. Based on the relative abundance of the statistically significant environmental indicator species and type of habitat of the most closely related phylotypes or cultivars, the majority (60–90%) of the OTUs in ES3 represented coastal marine plankton (Fig. 1*H*). Lacustrine species composed ~5% of the OTUs, but declined below the limit of detection (<0.01%) in sediments younger than ~5.2 ka cal B.P. The remainder of the OTUs (mainly land plants) were of terrestrial origin (Fig. 1*J*). Indicator species C25 (Fig. 3), with identical sequence to an uncultured *Nannochloropsis* (eustigmatophytes) from the moderately eutrophic Picnic Pond in Minnesota, was already present during the deposition of the calcite-rich Unit III-C1 lacustrine sediments of ES4 (IV = 28), but proved to be a better indicator species for the early marine ES3 (IV = 66). Cercozoa related to coastal marine clones (e.g., C32; Fig. 3) was another dominant group (16% of indicator species) during the

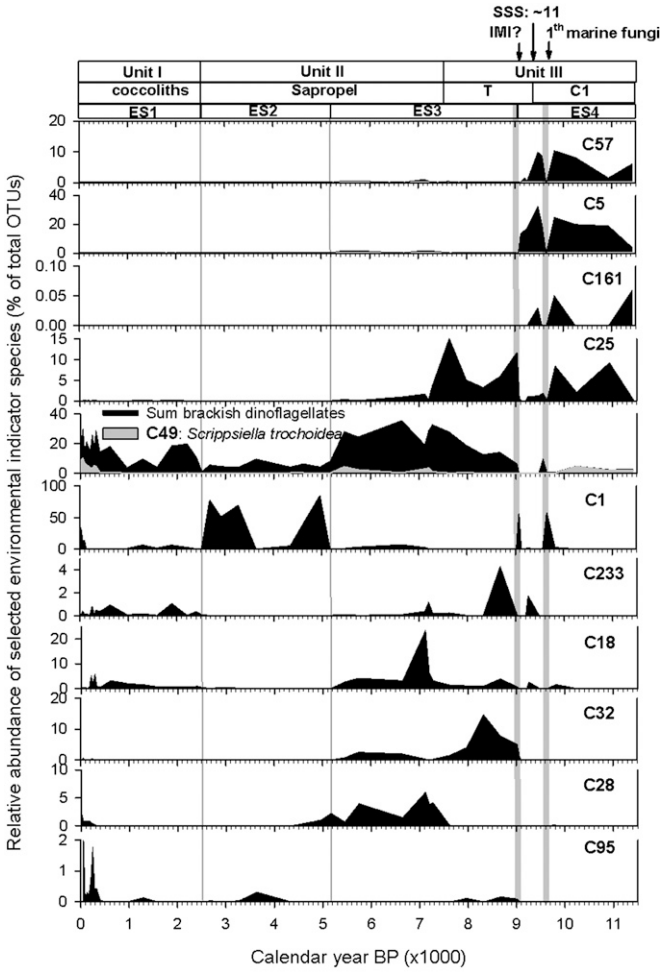

Fig. 3. Normalized relative abundance of selected highly relevant indicator species for the four environmental stages. Information on the most similar sequences is provided in the text. The phylogenetic affiliation with the most closely related GenBank sequences is shown in *SI Appendix*, Figs. S5–S9. Previously published IMI events (6) and the initial occurrence of the marine ascomycete fungus OTU C1 are shown above the figure. The sharp initial *E. huxleyi* peak (represented by OTU C233) at ~9.3 ka cal B.P. designates a salinity threshold of 11 ppt.

early ES3. However, coastal dinoflagellates represented the most diverse (51% of indicator species) plankton group for ES3 and gradually reached their highest relative abundance at the peak of the climate optimum during early to mid sapropel deposition (Fig. 3). For example, *S. trochoidea* also reappeared during early sapropel deposition and reached a relative abundance similar to that seen during ES4 (Fig. 3). Stramenopiles other than eustigmatophytes, including a brackish silicoflagellate (OTU C18) with an identical sequence as *Pseudopedinella elastica* and OTU C28 with an identical sequence to clone PF1E3H4 from a coastal upwelling zone, were also representative of the mid to late ES3 (Fig. 3 and *SI Appendix*, Figs. S3, S4, and S9 and Table S3).

A third major change in the community composition and a steep drop in the species richness occurred at ~5.2 ka cal B.P., at the onset of the dry and cooler Subboreal climate (Fig. 1*F*). The most abundant phylotypes were marine and terrestrial fungi (Fig. 1*I*). Notably, the marine fungus (OTU C1), which first occurred during ES4 at ~9.6 and 9.0 ka cal B.P., represented the best indicator species (IV = 54, $P = 0.01$) for ES2 (Fig. 3 and *SI Appendix*, Table S3). Furthermore, the relative abundance and diversity of dinoflagellates were lower than during ES3 (*SI Appendix*, Figs. S3 and S6). Metazoans other than copepods were relatively abundant (*SI Appendix*, Fig. S3*G*), but were not found to be statistically significant indicator species for ES2 ($P > 0.05$ in ISA). Copepods such as *Calanus*, which were continuously present according to the sensitive, targeted copepod 18S rRNA gene survey (Fig. 1*E*), represented only a small fraction of the total pool of 18S rRNA gene pyrotags and were not statistically significant indicator species for ES2 owing to their scattered distribution.

In the fresher ES1, fungi still composed up to 50% of the total eukaryote OTUs, but the majority of the fungal OTUs were no longer statistically significant representatives of this stage (*SI Appendix*, Fig. S3*D*). Plankton diversity started to increase in ES1 over the last millennium, eventually reaching levels similar to those seen in ES3, and coastal dinoflagellates returned to predominance (59% of indicator species) in ES1 (Fig. 3). The majority of these dinoflagellates were not present during older environmental stages (*SI Appendix*, Fig. S6 and Table S3), with the notable exception of *S. trochoidea*, which made a comeback in the last millennium and has gradually increased in abundance over the last ~400 y (Fig. 3). Despite their presence in older parts of the core, *S. trochoidea* as well as *E. huxleyi* showed the highest indicator values for ES1 (Fig. 3 and *SI Appendix*, Table S3). The coastal diatom *Skeletonema* (C95; Fig. 3) was occasionally detected in sediments as old as 9 ka cal B.P., and fish pathogens (ichthyosporea) (*SI Appendix*, Fig. S3*F*) first occurred during the peak of the climatic optimum, but their relative abundance increased mainly over the last four centuries. Chrysophytes (i.e., C80, related to clone LC109.90 from Taihu Lake, China) increased most dramatically over the last few decades (*SI Appendix*, Figs. S4 and S9).

Potential Bias of the Paleogenetics Approach. DNA damage accumulates over time owing to such factors as microbial enzymatic decomposition, as well as spontaneous abiotic hydrolysis and oxidation (37). The majority of these processes lead to strand breaks. To minimize PCR bias caused by strand breaks, only relatively short fragments (~100–500 bp) should be analyzed from Holocene sediments (18). Such PCR bias was minimal in our study, at least during the last 7,500 y, as demonstrated by the relatively constant ratio between the amount of similar-length DNA fragments and refractory alkenone lipid biomarkers from *E. huxleyi* (17). Hydrolytic and oxidative damage of ancient DNA is also known to lead to base pair substitutions and sequencing errors in ancient specimens (37), and thus to a possible overestimation of diversity. However, this form of bias was most likely minor throughout the 11,400-y record, given that high-quality bidirectional capillary sequencing of individual copepod (Fig. 1*E* and *SI Appendix*, Fig. S1) and *E. huxleyi* DGGE bands (17) yielded OTUs with identical sequences rather than numerous very closely related sequences.

Preservation of DNA is thought to be enhanced in taxa that produce resting stages (spores and cysts) (38), but the majority of DNA in marine sediments was found to be extracellular (20), and adsorption to minerals and organic particles increases the preservation potential of the extracellular DNA pool (39). Furthermore, DNA repair could prolong DNA preservation in dormant cells (38), but this could lead to a more efficient PCR amplification and overestimation of taxa that maintained intact genomes in this way after burial. This might explain, for example, the very high relative abundance of the marine fungal OTU C1 in our record. Indeed, various marine fungi were cultivated from up to 0.43 million y-old Indian Ocean sediments, and the majority of the fungal biomass was not present in the form of spores (40). Additional evidence of the preservation of intact fungi in ancient sediments comes from fungal rRNA that was detected in 0.3–2.8 million y-old sediments (41). Species-specific differences in gene copy numbers (42) also could have contributed to quantitative bias.

Despite these uncertainties, our paleogenetics approach successfully identified many taxa that previously escaped microscopic identification, and the evolution of the plankton paleome from the Deglacial to the Anthropocene accurately followed the

evolution of environmental changes in the Black Sea inferred from paired geochemical proxies.

Paleome-Inferred Climate and Environmental Conditions. In the Northern Hemisphere, despite high summer insolation, the presence of a remnant North American ice sheet maintained relatively cool and dry conditions during the Preboreal (~11.6–9 ka) (29). A sea level lower than the present level is thought to have hindered the marine connection until ~9 ka cal B.P., but whether the Black Sea was fresh or brackish is a matter of ongoing debate. Our paleome revealed that the majority of the environmental indicator taxa were freshwater plankton, whereas a small fraction of the DNA was derived from marine taxa that prevailed both before and after the presumed IMI at 9.0 ka cal B.P. For example, the first occurrence of *E. huxleyi* DNA at ~9.3 ka cal B.P. suggests that the Black Sea was already brackish up to 300 y before the previously documented IMI (6). Its first appearance at the Unit III–C1/T boundary could mark a threshold salinity of 11 ppt, considering, to the best of our knowledge, *E. huxleyi* has never been reported in settings with lower salinity. In addition, the initial short-term high relative abundance of the marine ascomycete fungus (OTU C1) at ~9.6 ka cal B.P. coincides with the timing of an initial increase in the $^{87}Sr/^{86}Sr$ ratio before this ratio became indicative of a continuous marine influence after 9.0 ka cal B.P. (5). Both markers suggest a marine inflow into the Black Sea in the Unit III C1 interval, centuries earlier than reported previously (6).

Of note, the ascomycete fungus with an identical sequence to species inhabiting the marine oxygen minimum zone could have been derived from the Sea of Marmara, which was already stratified at that time (43). The presence of *S. trochoidea* DNA in the Unit III C1 interval suggests a marine influence even before ~9.6 ka cal B.P. Furthermore, *S. trochoidea* was present during mid to late sapropel formation, and once again became relatively abundant during the last few centuries (Fig. 3 and *SI Appendix*, Fig. S6). The recently observed return of massive red tide blooms of *S. trochoidea* in the Black Sea is attributed to an anthropogenic increase in nutrient loads to the basin (44). The presence of DNA of a species that indicates eutrophic conditions in the ES4 sediments supports the idea that the $CaCO_3$ maximum in Unit III (Fig. 1*A*) was deposited under high-nutrient, high-productivity conditions during the Preboreal (45).

With almost-complete ice sheet melting, continued high summer insolation led to the warm and moist conditions of the mid-Holocene climatic optimum (~9–5 ka cal B.P.; ES3), which is most obvious in Northern Europe (29). The data presented here, along with a previously reported 18S rRNA gene clone library from northwestern Black Sea sediments (20), show a gradual shift from oligotrophic to more eutrophic conditions in the Black Sea during ES3. This shift is represented by a relatively high abundance of the *Nannochloropsis*-related eustigmatophyte from the dystrophic Tower Pond (46) and a shift to a predominance of coastal dinoflagellates including *S. scrippsiella*, as well as uncultured stramenopiles, cercozoans, and ichthyosporea related to species from nutrient-rich coastal environments after ~7 ka cal B.P. The shift from a dystrophic to more eutrophic community structure during ES3 occurred at the peak of the climatic optimum, when increased precipitation could have resulted in a shoaling of the chemocline that brought nutrients into the photic zone, according to recent geochemical studies (47, 48).

ES2 represents the cooler and drier Subboreal (29), as indicated by the gradual decrease in SST and steep increase in SSS between ca. 5.2 and 2.5 ka cal B.P. (Fig. 1). This period also saw a drastic decrease in overall plankton diversity and a return of a high relative abundance of the marine ascomycete fungus that initially peaked at the revised IMI at ~9.6 ka cal B.P. Interestingly, the distribution of the fungus between ~5.2 and 2.5 ka cal B.P. is comparable to the downcore distribution of the cyanobacterial aridity marker scytonemin in other Subboreal sediments of the Black Sea (47). Previous geochemical evidence suggests that during this time interval, the water column remained redox-stratified, but the chemocline was deeper than during the climatic optimum (47, 48). This resulted in decreased nutrients in the photic zone, as indicated by the lower relative abundance of dinoflagellates, including the absence of *S. trochoidea* during ES2. Both fungal DNA and scytonemin were at minimum levels at ~3.5–4.5 ka cal B.P., whereas our paleome record revealed a simultaneous increase in the relative abundance of terrestrial indicator taxa (Fig. 1*J*), suggesting that the drier conditions of the Subboreal in this region were interrupted by a period of higher precipitation and runoff.

The timing of the late Holocene basin-wide freshening (ES1) closely coincides with the onset of the cool and wet Subatlantic climate interval (29). The combined climatic factors and increased anthropogenic land use during this period led to expansion of the Danube delta as a result of the increased fluvial influx into the Black Sea (24). The Danube River, draining ~30% of central and Eastern Europe, provides more than 60% of the entire runoff reaching the Black Sea. Because fluvial nutrients feed the surface mixed layer that accounts for only 13% of the entire basin volume, there is a strong coupling between Danube fluxes and the Black Sea's biogeochemistry and ecology (24). The increased terrestrial runoff during the refreshening of the Black Sea could explain the increase in the relative abundance of fungi derived from disturbed soils in the watershed during ES1 (*SI Appendix*, Fig. S3*D*). The increased terrestrial freshwater and nutrient runoff during ES1 also caused a return to a plankton community dominated by dinoflagellates (*SI Appendix*, Fig. S3*A*). However, unlike in the other environmental stages, the complex land use modifications in the Black Sea's watershed during ES1 resulted in a cascade of successive changes in the overall plankton community structure over the last millennium (Fig. 2*A*). The greatest changes in the overall community structure occurred over the last century (as shown by NMDS clustering of the youngest three samples) as the fluvial biogeochemical influx was drastically modified through combined watershed land use and pollution and river engineering as the Industrial Revolution accelerated in the early 20th century (24).

Final Note. This study shows that relatively long DNA fragments of past plankton species were preserved not only in the TOC-rich sapropel and Unit I sediments, but also in the TOC-poor lacustrine and early marine sediments, which were deposited under fully oxygenated conditions. Although the anoxic Cariaco Basin is a suitable next candidate for paleomic research, plankton DNA likely is much more widely preserved in Quaternary marine and lacustrine sediments than previously thought. Thus, the reconstruction of paleomes, in combination with more traditional paleoecology proxies, could greatly diversify our knowledge of past ecosystems and paleoenvironments in general.

Materials and Methods

Detailed information on sampling locations and subsampling of sediment intervals for the geochemical and molecular lipid and DNA analysis are provided in *SI Appendix*. The age model, total DNA extraction, and geochemical analysis (XRF calcium, TOC, and extraction and identification of alkenones and their use for temperature and salinity reconstructions) for the Unit I and II intervals have been described in detail elsewhere (17, 24) and were extended for the lacustrine sediment intervals for this study. Details of the paleomic approach and the statistical interpretation of the data are provided in *SI Appendix*.

ACKNOWLEDGMENTS. We thank Tzu Hsuan Yang for laboratory assistance. This study was supported by National Science Foundation Grants OCE 0602423 (to M.J.L.C.), OCE 0825020 (to M.J.L.C.), and EAR 0952146 (to L.G.) and by the Woods Hole Oceanographic Institution.

1. Ross DA, Degens ET, Macilvaine J (1970) Black Sea: Recent sedimentary history. *Science* 170(3954):163–165.

2. Ryan WBF, Major CO, Lericolais G, Goldstein SL (2003) Catastrophic flooding of the Black Sea. *Annu Rev Earth Planet Sci* 31:525–554.

3. Giosan L, Filip F, Constatinescu S (2009) Was the Black Sea catastrophically flooded in the early Holocene? *Quat Sci Rev* 28(1-2):1–6.
4. Hiscott RN, et al. (2007) A gradual drowning of the southwestern Black Sea shelf: Evidence for a progressive rather than abrupt Holocene reconnection with the eastern Mediterranean Sea through the Marmara Sea gateway. *Quat Int* 167:19–34.
5. Major CO, et al. (2006) The co-evolution of Black Sea level and composition through the last deglaciation and its paleoclimatic significance. *Quat Sci Rev* 25(17-18): 2031–2047.
6. Soulet G, Menot G, Lericolais G, Bard E (2011) A revised calendar age for the last reconnection of the Black Sea to the global ocean. *Quat Sci Rev* 30(9-10):1019–1026.
7. Soulet G, et al. (2010) Glacial hydrologic conditions in the Black Sea reconstructed using geochemical pore water profiles. *Earth Planet Sci Lett* 296(1-2):57–66.
8. Marret F, Mudie P, Aksu A, Hiscott RN (2009) A Holocene dinocyst record of a two-step transformation of the Neoeuxinian brackish water lake into the Black Sea. *Quat Int* 197:72–86.
9. Major C, Ryan W, Lericolais G, Hajdas I (2002) Constraints on Black Sea outflow to the Sea of Marmara during the last glacial–interglacial transition. *Mar Geol* 190(1-2): 19–34.
10. Bahr A, Arz HW, Lamy F, Wefer G (2006) Late glacial to Holocene paleoenvironmental evolution of the Black Sea, reconstructed with stable oxygen isotope records obtained on ostracod shells. *Earth Planet Sci Lett* 241(3-4):863–875.
11. Giunta S, Morigi C, Negri A, Guichard F, Lericolais G (2007) Holocene biostratigraphy and paleoenvironmental changes in the Black Sea based on calcareous nannoplankton. *Mar Micropaleontol* 63(1-2):91–110.
12. Filipova-Marinova M, Pavlov D, Coolen MJL, Giosan L (2013) First high-resolution marinopalynological stratigraphy of Late Quaternary sediments from the central part of the Bulgarian Black Sea area. *Quat Int* 293:170–183.
13. Bahr A, Lamy F, Arz H, Kuhlmann H, Wefer G (2005) Late glacial to Holocene climate and sedimentation history in the NW Black Sea. *Mar Geol* 214:309–322.
14. Dale B (1983) Dinoflagellate resting cysts: "Benthic plankton." *Survival Strategies of the Algae*, ed Fryxel GA (Cambridge Univ Press, Cambridge, UK), pp 69–137.
15. Inagaki F, Okada H, Tsapin AI, Nealson KH (2005) Microbial survival. The paleome: A sedimentary genetic record of past microbial communities. *Astrobiology* 5(2): 141–153.
16. Bissett A, Gibson JAE, Jarman SN, Swadling KM, Cromer L (2005) Isolation, amplification, and identification of ancient copepod DNA from lake sediments. *Limnol Oceanogr Methods* 3:533–542.
17. Coolen MJL, et al. (2009) DNA and lipid molecular stratigraphic records of haptophyte succession in the Black Sea during the Holocene. *Earth Planet Sci Lett* 284(3-4): 610–621.
18. Boere AC, Sinninghe Damsté JS, Rijpstra WIC, Volkman JK, Coolen MJL (2011) Source-specific variability in post-depositional DNA preservation with potential implications for DNA-based paleoecological records. *Org Geochem* 42(10):1216–1225.
19. Coolen MJL (2011) 7000 years of *Emiliania huxleyi* viruses in the Black Sea. *Science* 333(6041):451–452.
20. Corinaldesi C, Barucca M, Luna GM, Dell'Anno A (2011) Preservation, origin and genetic imprint of extracellular DNA in permanently anoxic deep-sea sediments. *Mol Ecol* 20(3):642–654.
21. Margulies M, et al. (2005) Genome sequencing in microfabricated high-density picolitre reactors. *Nature* 437(7057):376–380.
22. Muyzer G, de Waal EC, Uitterlinden AG (1993) Profiling of complex microbial populations by denaturing gradient gel electrophoresis analysis of polymerase chain reaction-amplified genes coding for 16S rRNA. *Appl Environ Microbiol* 59(3):695–700.
23. Van der Meer MTJ, et al. (2008) Molecular isotopic and dinoflagellate evidence for late Holocene freshening of the Black Sea. *Earth Planet Sci Lett* 267:426–434.
24. Giosan L, et al. (2012) Early anthropogenic transformation of the Danube–Black Sea system. *Sci Rep* 2:582.
25. Eglinton TI, et al. (1997) Variability in radiocarbon ages of individual organic compounds from marine sediments. *Science* 277:796–799.
26. Jones GA, Gagnon AR (1994) Radiocarbon chronology of Black Sea sediments. *Deep Sea Res Part I Oceanogr Res Pap* 41(3):531–557.
27. Hay BJ (1988) Sediment accumulation in the central western Black Sea over the past 5100 years. *Paleoceanography* 3(4):491–508.
28. Arthur MA, et al. (1994) Varve calibration records of carbonate and organic carbon accumulation over the last 2000 years in the Black Sea. *Global Biogeochem Cycles* 8(2): 195–217.
29. Wanner H, et al. (2008) Mid- to Late Holocene climate change: An overview. *Quat Sci Rev* 27(19-20):1791–1828.
30. Marcus NH (1996) Ecological and evolutionary significance of resting eggs in marine copepods: Past, present, and future studies. *Hydrobiologia* 320(1-3):141–152.
31. Svetlichny L, et al. (2010) Salinity tolerance of *Calanus euxinus* in the Black and Marmara Seas. *Mar Ecol Prog Ser* 404:127–138.
32. Xu L, et al. (2001) Identification of a novel alkenone in Black Sea sediments. *Org Geochem* 32:633–645.
33. Everhart SE, Keller HW, Ely JS (2008) Influence of bark pH on the occurrence and distribution of tree canopy myxomycete species. *Mycologia* 100(2):191–204.
34. Zonneveld KAF, Versteegh GJM, De Lange GJ (2001) Palaeoproductivity and post-depositional aerobic organic matter decay reflected by dinoflagellate cyst assemblages of the Eastern Mediterranean S1 sapropel. *Mar Geol* 172(3-4):181–195.
35. Jebaraj CS, Raghukumar C, Behnke A, Stoeck T (2010) Fungal diversity in oxygen-depleted regions of the Arabian Sea revealed by targeted environmental sequencing combined with cultivation. *FEMS Microbiol Ecol* 71(3):399–412.
36. Ross DA, Degens ET (1974) Recent sediments of Black Sea. *AAPG Bull* 20:183–199.
37. Willerslev E, Cooper A (2005) Ancient DNA. *Proc Biol Sci* 272(1558):3–16.
38. Johnson SS, et al. (2007) Ancient bacteria show evidence of DNA repair. *Proc Natl Acad Sci USA* 104(36):14401–14405.
39. Coolen MJL, Overmann J (2007) 217 000-year-old DNA sequences of green sulfur bacteria in Mediterranean sapropels and their implications for the reconstruction of the paleoenvironment. *Environ Microbiol* 9(1):238–249.
40. Raghlukumar C, et al. (2004) Buried in time: Culturable fungi in a deep-sea sediment core from the Chagos Trench, Indian Ocean. *Deep Sea Res Part I Oceanogr Res Pap* 51(11):1759–1768.
41. Orsi W, Biddle JF, Edgcomb V (2013) Deep sequencing of subseafloor eukaryotic rRNA reveals active fungi across marine subsurface provinces. *PLoS ONE* 8(2):e56335.
42. Hou YB, Lin SJ (2009) Distinct gene number-genome size relationships for eukaryotes and non-eukaryotes: Gene content estimation for dinoflagellate genomes. *PLoS ONE* 4(9):e6978.
43. Vidal L, et al. (2010) Hydrology in the Sea of Marmara during the last 23 ka: Implications for timing of Black Sea connections and sapropel deposition. *Paleoceanography* 25:PA1205.
44. Bodeneau N (1993) *Microalgal Blooms in the Romanian Area of the Black Sea and Contemporary Eutrophication Conditions* (Elsevier, Amsterdam).
45. Soulet G, et al. (2011) Black Sea "lake" reservoir age evolution since the Last Glacial: Hydrologic and climatic implications. *Earth Planet Sci Lett* 308(1-2):245–258.
46. Fawley MW, Fawley KP, Buchheim MA (2004) Molecular diversity among communities of freshwater microchlorophytes. *Microb Ecol* 48(4):489–499.
47. Fulton JM, Arthur MA, Freeman KH (2012) Subboreal aridity and scytonemin in the Holocene Black Sea. *Org Geochem* 49:47–55.
48. Huang Y, Freeman KH, Wilkin RT, Arthur MA, Jones AD (2000) Black Sea chemocline oscillations during the Holocene: Molecular and isotopic studies of marginal sediments. *Org Geochem* 31:1525–1531.